

# Occupation probability for acceptor in Al-implanted *p*-type 4H-SiC

Hideharu Matsuura,<sup>a)</sup> Koichi Sugiyama, Kazuhiro Nishikawa, Takashi Nagata, and Nobuya Fukunaga

*Department of Electronic Engineering and Computer Science, Osaka Electro-Communication University, 18-8 Hatsu-cho, Neyagawa, Osaka 572-8530, Japan*

(Received 17 January 2003; accepted 12 May 2003)

Al-implanted *p*-type 4H-SiC layers with different implantation and annealing temperatures are formed, and the temperature dependence of the hole concentration  $p(T)$  is obtained by Hall-effect measurements. The Al acceptor level in SiC is deep ( $\sim 180$  meV), and its first excited state level calculated by the hydrogenic model is still deep ( $\sim 35$  meV), which is close to the acceptor level of B in Si. Therefore, in order to determine the reliable acceptor density ( $N_A$ ) from  $p(T)$ , the Fermi-Dirac distribution function is not appropriate for Al acceptors in SiC, and a distribution function including the influence of the excited states of the Al acceptor is required. It is demonstrated that the proposed distribution function is suitable for obtaining the actual relationship between  $N_A$  and  $p(T)$  in *p*-type 4H-SiC. © 2003 American Institute of Physics.

[DOI: 10.1063/1.1589176]

## I. INTRODUCTION

Silicon carbide (SiC) has been an attractive semiconductor because of a wide band gap, high electron mobility, a high electron-saturation-drift velocity and a high thermal conductivity. As a result, it has been regarded as a promising semiconductor for devices operating at high powers, high frequencies, and high temperatures. Since these devices are operated in a wide temperature range, the relationship between a dopant density and a temperature dependence of the majority-carrier concentration in SiC becomes important for device simulation. Here, this relationship indicates a distribution function (i.e., occupation probability) of electrons or holes for dopants. The Poisson equation plays an important role in the device simulation, and it requires an accurate dopant density and a distribution function for the dopant.

Excited states of substitutional dopants in semiconductors have been theoretically discussed using the hydrogenic model,<sup>1-3</sup> and the existence of the excited states of dopants (e.g., B, P) in Si or Ge has been experimentally confirmed from infrared absorption measurements at very low temperatures.<sup>1,4-8</sup> However, the influence of the excited states on the majority-carrier concentration in Si or Ge has not been experimentally confirmed because the excited state levels of the dopants in Si or Ge are too close to the allowed band edge, that is, the valence band maximum ( $E_V$ ) or the conduction band minimum ( $E_C$ ).

Because of a dielectric constant ( $\epsilon_s$ ) of SiC lower than that of Si and because of a hole-effective mass ( $m_h^*$ ) of SiC heavier than its electron-effective mass ( $m_e^*$ ), the ground-state level ( $\Delta E_1$ ) of a substitutional acceptor in SiC becomes large according to the hydrogenic model, which is calculated to be approximately 136 meV. Here,  $\Delta E_1$  is called the theoretical value of an acceptor level ( $\Delta E_A$ ), which is measured from  $E_V$ . The experimental  $\Delta E_A$  was reported to be

$\sim 180$  meV from photoluminescence (PL) studies,<sup>9</sup> suggesting that central cell corrections<sup>10</sup> make the experimental  $\Delta E_A$  larger than  $\Delta E_1$ . Since the theoretical first excited state level ( $\Delta E_2$ ) of the acceptor in SiC is close to  $\Delta E_A$  ( $\sim 45$  meV) of B in Si, the excited states of Al acceptors in SiC must affect the hole concentration, indicating that a suitable distribution function including the influence of the excited states should be required to investigate the relationship between the acceptor density ( $N_A$ ) and the temperature dependence of the hole concentration  $p(T)$ .

Using the Fermi-Dirac distribution function  $f_{FD}(\Delta E_A)$  that does not include the influence of the excited states of acceptors, almost all of the researchers have determined  $\Delta E_A$ ,  $N_A$  and the compensating density ( $N_{comp}$ ) in Al-doped or Al-implanted SiC by a least-squares fit of the charge neutrality equation to  $p(T)$  experimentally obtained from Hall-effect measurements.<sup>11-13</sup> However, the value of  $N_A$  determined using  $f_{FD}(\Delta E_A)$  has been always much higher than the concentration of Al atoms ( $C_{Al}$ ), which is determined by secondary ion mass spectroscopy.<sup>11-15</sup> This suggests that the obtained  $N_A$  should not be reliable because  $N_A$ , which means the density of Al atoms located at the substitutional sites in SiC, must be less than or equal to  $C_{Al}$ . The situation in Mg-doped *p*-type GaN has also been the same.<sup>16</sup>

The following two attempts were made to determine the reliable  $N_A$  from Hall-effect measurements; (1) the experimental adjustment of Hall-scattering factor for holes ( $\gamma_H$ ) and (2) the theoretical introduction of a distribution function suitable for Al acceptors. Pensl has strongly insisted that  $\gamma_H$  should be temperature dependent (0.5–1.2).<sup>13</sup> On the other hand, there are two types of reported distribution functions including the influence: (a) the conventional distribution function  $f_{conv}(\Delta E_A)$  appearing in books,<sup>17-19</sup> and (b) the distribution function  $f(\Delta E_A)$  that we have proposed.<sup>14,15</sup> According to  $f_{conv}(\Delta E_A)$ , since the excited states behave just like a hole trap,  $N_A$  determined using  $f_{conv}(\Delta E_A)$  is much

<sup>a)</sup> Author to whom correspondence should be addressed; electronic mail: matsuura@isc.osakac.ac.jp

higher than  $N_A$  determined using  $f_{FD}(\Delta E_A)$ . In order to obtain the reliable  $N_A$  from  $p(T)$ , therefore, we have proposed  $f(\Delta E_A)$  and have been theoretically and experimentally testing it.<sup>14,15</sup>

In this article, from a viewpoint of the introduction of the distribution function, we determine  $N_A$ ,  $\Delta E_A$  and  $N_{comp}$  in several Al-implanted  $p$ -type 4H-SiC layers with different implantation temperatures ( $T_{implant}$ ) and annealing temperatures ( $T_{anneal}$ ) from  $p(T)$ .

## II. DISTRIBUTION FUNCTIONS FOR DEEP DOPANTS

When the influence of the excited states of acceptors on  $p(T)$  is neglected because of small  $\Delta E_A$ ,  $f_{FD}(\Delta E_A)$  can be

made use of. The value of this distribution function at  $\Delta E_A$  is described as<sup>20</sup>

$$f_{FD}(\Delta E_A) = \frac{1}{1 + 4 \exp\left(\frac{\Delta E_A - \Delta E_F(T)}{kT}\right)}, \quad (1)$$

where  $\Delta E_F(T)$  is the Fermi level measured from  $E_V$  at  $T$ ,  $k$  is the Boltzmann constant, and  $T$  is the absolute temperature.

On the other hand, we have proposed a distribution function including the influence, which is given by<sup>14,15</sup>

$$f(\Delta E_A) = \frac{1}{1 + 4 \exp\left(-\frac{E_{ex}(T)}{kT}\right) \left[ \exp\left(\frac{\Delta E_A - \Delta E_F(T)}{kT}\right) + \sum_{r=2} g_r \exp\left(\frac{\Delta E_r - \Delta E_F(T)}{kT}\right) \right]}, \quad (2)$$

where  $\Delta E_r$  is the  $(r-1)$ th excited state level measured from  $E_V$ , which is described as

$$\Delta E_r = \frac{q^4 m_h^*}{8h^2 \epsilon_0^2 \epsilon_s^2 r^2} = 13.6 \frac{m_h^*}{m_0 \epsilon_s^2 r^2} \text{ (eV)} \quad (3)$$

according to the hydrogenic model,<sup>1-3</sup>  $\overline{E_{ex}(T)}$  is an ensemble average of the ground ( $r=1$ ) and excited state ( $r \geq 2$ ) levels of the acceptor measured from  $\Delta E_A$ , which is given by<sup>14,15,21</sup>

$$\overline{E_{ex}(T)} = \frac{\sum_{r=2} (\Delta E_A - \Delta E_r) g_r \exp\left(-\frac{\Delta E_A - \Delta E_r}{kT}\right)}{1 + \sum_{r=2} g_r \exp\left(-\frac{\Delta E_A - \Delta E_r}{kT}\right)}, \quad (4)$$

where  $g_r$  is the  $(r-1)$ th excited state degeneracy factor described as<sup>1,17</sup>

$$g_r = r^2, \quad (5)$$

$q$  is the electron charge,  $m_0$  is the free-space electron mass,  $h$  is Planck's constant, and  $\epsilon_0$  is the free-space permittivity.

An average acceptor level  $\overline{\Delta E_A(T)}$  is defined by<sup>14,15</sup>

$$\overline{\Delta E_A(T)} \equiv \Delta E_A - \overline{E_{ex}(T)}. \quad (6)$$

Since the Bohr radius ( $a^*$ ) of the ground state, which is given by<sup>2,3</sup>

$$a^* = \frac{\epsilon_0 \epsilon_s h^2}{\pi m_h^* q^2} = 0.53 \frac{m_0 \epsilon_s}{m_h^*} \text{ (\AA)}, \quad (7)$$

is very small in this case, the experimental  $\Delta E_A$  becomes larger than the theoretical  $\Delta E_1$  as follows:

$$\Delta E_A = \Delta E_1 + E_{CCC}, \quad (8)$$

where  $E_{CCC}$  is the energy induced due to central cell corrections.<sup>10</sup> Since the wave function extension of the  $(r-1)$ th excited state is of order  $r^2 a^*$ ,<sup>2</sup> however, the excited state levels are considered not to be affected by central cell corrections.<sup>22</sup>

Moreover,  $f_{conv}(\Delta E_A)$  was reported to be described as<sup>17-19</sup>

$$f_{conv}(\Delta E_A) = \frac{1}{1 + 4 \left[ \exp\left(\frac{\Delta E_A - \Delta E_F(T)}{kT}\right) + \sum_{r=2} g_r \exp\left(\frac{\Delta E_r - \Delta E_F(T)}{kT}\right) \right]}. \quad (9)$$

In comparison to Eq. (2),  $f_{\text{conv}}(\Delta E_A)$  ignores  $\overline{E_{\text{ex}}(T)}$ . This indicates that the ionization efficiency of acceptors in  $f_{\text{conv}}(\Delta E_A)$  should be much less than that in  $f(\Delta E_A)$  or  $f_{\text{FD}}(\Delta E_A)$ .

### III. FREE CARRIER CONCENTRATION SPECTROSCOPY

Free carrier concentration spectroscopy (FCCS) is a graphical peak analysis method for determining the densities and energy levels of impurities and defects in a semiconductor even when several types of impurity species and defects are considered to be included.<sup>14,15,23–27</sup> Using an experimental  $p(T)$ , the FCCS signal is defined as

$$H(T, E_{\text{ref}}) \equiv \frac{p(T)^2}{(kT)^{5/2}} \exp\left(\frac{E_{\text{ref}}}{kT}\right). \quad (10)$$

The FCCS signal has a peak at the temperature corresponding to each acceptor level or hole-trap level, where  $E_{\text{ref}}$  is the parameter that can shift the peak temperature of  $H(T, E_{\text{ref}})$  within the temperature range of the measurement, which is discussed later. From each peak value and peak temperature, the density and energy level of the corresponding acceptor or hole trap can be accurately determined.

Although FCCS can be applied in any nondegenerate semiconductor including several types of acceptor species, donor species and traps, we here focus on a  $p$ -type semiconductor doped with one sort of acceptor. From the neutrality condition,  $p(T)$  is given by

$$p(T) = N_A F(\Delta E_A) - N_{\text{comp}} \quad (11)$$

in the temperature range in which the electron concentration  $n(T)$  is much less than  $p(T)$ , where  $F(\Delta E_A)$  represents  $f_{\text{FD}}(\Delta E_A)$  or  $f_{\text{conv}}(\Delta E_A)$  or  $f(\Delta E_A)$ . In the case of nondegenerate semiconductors, furthermore,  $p(T)$  is given by<sup>28</sup>

$$p(T) = N_V(T) \exp\left(-\frac{\Delta E_F(T)}{kT}\right), \quad (12)$$

where

$$N_V(T) = N_{V0} k^{3/2} T^{3/2} \quad (13)$$

and

$$N_{V0} = 2 \left( \frac{2\pi m_h^*}{h^2} \right)^{3/2}. \quad (14)$$

Substituting Eq. (11) for one of the two  $p(T)$  in Eq. (10) and substituting Eq. (12) for the other  $p(T)$  in Eq. (10) yields

$$H(T, E_{\text{ref}}) = \frac{N_A}{kT} \exp\left(-\frac{\Delta E_A - E_{\text{ref}}}{kT}\right) I(\Delta E_A) - \frac{N_{\text{comp}} N_{V0}}{kT} \exp\left(\frac{E_{\text{ref}} - \Delta E_F(T)}{kT}\right), \quad (15)$$

where

$$I(\Delta E_A) = N_{V0} \exp\left(\frac{\Delta E_A - \Delta E_F(T)}{kT}\right) F(\Delta E_A). \quad (16)$$

The function

$$\frac{N_A}{kT} \exp\left(-\frac{\Delta E_A - E_{\text{ref}}}{kT}\right) \quad (17)$$

in Eq. (15) has a peak value of  $N_A \exp(-1)/kT_{\text{peak}}$  at the peak temperature

$$T_{\text{peak}} = \frac{\Delta E_A - E_{\text{ref}}}{k}. \quad (18)$$

As is clear from Eq. (18),  $E_{\text{ref}}$  can shift the peak of  $H(T, E_{\text{ref}})$  within the temperature range of the measurement. Although the actual  $T_{\text{peak}}$  of  $H(T, E_{\text{ref}})$  is slightly different from  $T_{\text{peak}}$  calculated by Eq. (18) due to the temperature dependence of  $I(\Delta E_A)$ , we can easily determine the accurate values of  $N_A$  and  $\Delta E_A$  from the peak of the experimental  $H(T, E_{\text{ref}})$ , using a personal computer. The Windows application software for FCCS can be freely downloaded at our web site (<http://www.osakac.ac.jp/labs/matsuura/>).

When  $f_{\text{FD}}(\Delta E_A)$  is substituted for  $F(\Delta E_A)$  in Eq. (16), the values of  $N_A$ ,  $\Delta E_A$  and  $N_{\text{comp}}$  determined by FCCS coincide with those determined by the curve-fitting procedure of  $p(T)$  using  $f_{\text{FD}}(\Delta E_A)$ . In the following sections, therefore, FCCS is applied to determine  $N_A$ ,  $\Delta E_A$  and  $N_{\text{comp}}$  corresponding to  $f_{\text{FD}}(\Delta E_A)$  or  $f_{\text{conv}}(\Delta E_A)$  or  $f(\Delta E_A)$ .

### IV. EXPERIMENT

In order to form  $p$ -type 4H-SiC layers, Al ions were implanted at room temperature or 1000 °C to 5- $\mu\text{m}$ -thick  $n$ -type 4H-SiC epilayers with N atoms of  $2.5 \times 10^{15} \text{ cm}^{-3}$  on  $n$ -type 4H-SiC {0001} substrate with 8° off to  $\langle 11\bar{2}0 \rangle$  direction. In order to obtain a box profile of  $C_{\text{Al}}$ , sevenfold Al ion implantation was carried out with different energies onto the SiC epilayer surface tilted to 7° to normal. Each dose of Al ions was  $3.0 \times 10^{14} \text{ cm}^{-2}$ , and the implantation energies were 1.0, 1.6, 2.4, 3.3, 4.4, 5.6, and 7.0 meV. After the implantation, the sample was annealed at 1443 or 1575 °C for 1 h in an Ar atmosphere. The Rutherford backscattering spectroscopy (RBS) spectra were measured using 2 meV He ions. In this case, the deepest measurable depth in SiC was  $\sim 1 \mu\text{m}$  from the surface.

The 1.3- $\mu\text{m}$ -thick layer from the surface was removed by reactive ion etching using a mixture of  $\text{CF}_4$  and  $\text{O}_2$ , and then the sample was cut into a  $4 \times 4 \text{ mm}^2$  in size. Ohmic metal (Al/Ti) was deposited on four corners of the etched surface, and the sample was annealed. The  $p(T)$  in the  $p$ -type layer formed by the Al implantation was measured by the van der Pauw method in the temperature range of 100 and 420 K and in a magnetic field of 1.4 T.

### V. RESULTS

Figure 1 shows the profile of  $C_{\text{Al}}$  calculated by the Monte Carlo simulation program of the stopping and range of ions in matter (SRIM-2000) after Biersack,<sup>29</sup> where the density of SiC used in calculation was  $3.2 \text{ g/cm}^3$ .<sup>30</sup> From Fig. 1, the box profile of  $C_{\text{Al}}$  is confirmed, and the average  $C_{\text{Al}}$  in the  $p$  layer is  $\sim 1 \times 10^{19} \text{ cm}^{-3}$ .

Figure 2 shows the RBS spectra for the random and virgin samples, and samples implanted at room temperature or 1000 °C. The yield in the sample implanted at 1000 °C is

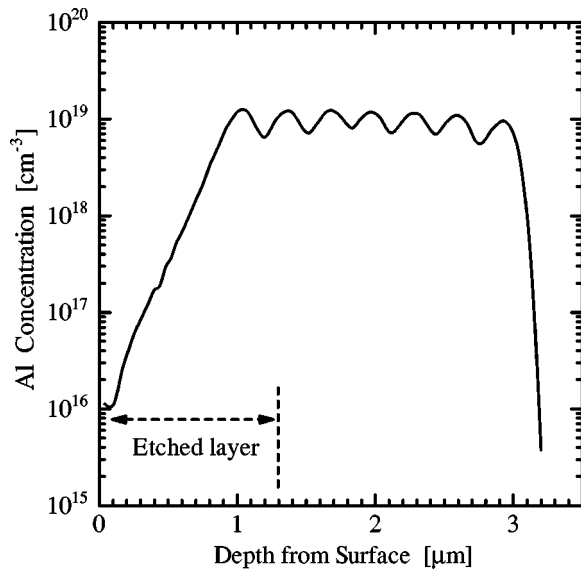


FIG. 1. Profile of Al concentration simulated by SRIM-2000.

substantially below that in the sample implanted at room temperature, indicating that the dynamic annealing during elevated temperature implantation prevented making SiC layers amorphous. The RBS spectra of the annealed samples were close to the virgin level, indicating that the damage due to the ion implantation was almost annealed out. Since Al atoms located at substitutional sites of SiC crystal can only act as an acceptor,  $N_A$  should be lower than or close to  $C_{Al}$  of  $\sim 1 \times 10^{19} \text{ cm}^{-3}$ .

Four *p*-type 4H-SiC layers with different  $T_{\text{implant}}$  and  $T_{\text{anneal}}$  were investigated, as shown in Table I. Figure 3 depicts four temperature dependences of the hole mobility  $\mu_p(T)$ . The solid circles, open circles, solid triangles, and open triangles represent  $\mu_p(T)$  for *p*SiC(HH), *p*SiC(HL), *p*SiC(LH), and *p*SiC(LL), respectively. Two  $\mu_p(T)$  for *p*SiC(HH) and *p*SiC(LH) are higher than those for *p*SiC(HL) and *p*SiC(LL), indicating that high  $T_{\text{anneal}}$  is ef-

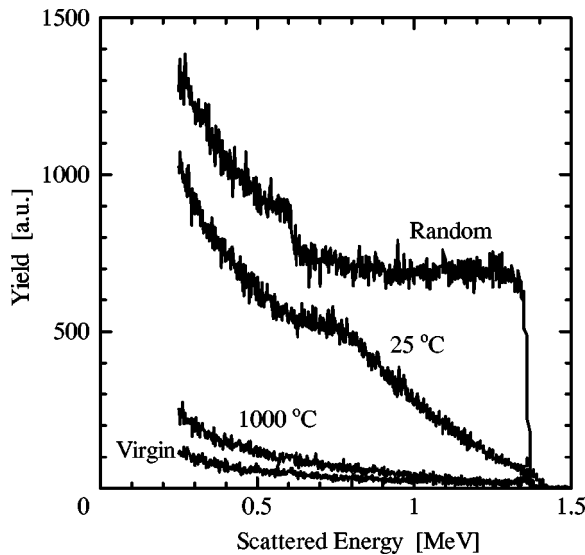


FIG. 2. RBS spectra for virgin and random samples, and samples implanted at room temperature or 1000 °C.

TABLE I. Sample preparation conditions.

Sample number	$T_{\text{implant}}$ (°C)	$T_{\text{anneal}}$ (°C)
<i>p</i> SiC(HH)	1000	1575
<i>p</i> SiC(HL)	1000	1443
<i>p</i> SiC(LH)	Room temperature	1575
<i>p</i> SiC(LL)	Room temperature	1443

fective on  $\mu_p(T)$ . In almost all of the measurement-temperature range, phonon scattering is considered to be dominant. Therefore, it is considered that  $\gamma_H$  is independent of  $T$ .

In general,  $\gamma_H = 3\pi/8 \approx 1.18$  for phonon scattering, while  $\gamma_H = 315\pi/512 \approx 1.93$  for ionized impurity scattering that is dominant at low temperatures.<sup>31</sup> In *p*-type Si,  $\gamma_H$  is theoretically derived to be  $\sim 0.73$  for optical-phonon scattering, while  $\gamma_H$  is  $\sim 1.43$  for acoustic-phonon scattering in *p*-type Ge.<sup>32</sup> Judging from these reports,  $\gamma_H = 1$  is not a bad assumption.

Figure 4 shows four  $p(T)$  obtained using  $\gamma_H = 1$ , where the relationship between  $p(T)$  and the experimentally obtained Hall coefficient ( $R_H$ ) is expressed as

$$R_H = \frac{\gamma_H}{qp(T)}. \quad (19)$$

The solid circles, open circles, solid triangles, and open triangles represent  $p(T)$  for *p*SiC(HH), *p*SiC(HL), *p*SiC(LH), and *p*SiC(LL), respectively. Two  $p(T)$  for *p*SiC(HH) and *p*SiC(LH) are higher than those for *p*SiC(HL) and *p*SiC(LL). While  $p(T)$  in *p*SiC(LH) is the highest at low temperatures,  $p(T)$  in *p*SiC(HH) is the highest at high temperatures.

Figure 5 shows four  $\Delta E_F(T)$  calculated using

$$\Delta E_F(T) = kT \ln \left[ \frac{N_V(T)}{p(T)} \right], \quad (20)$$

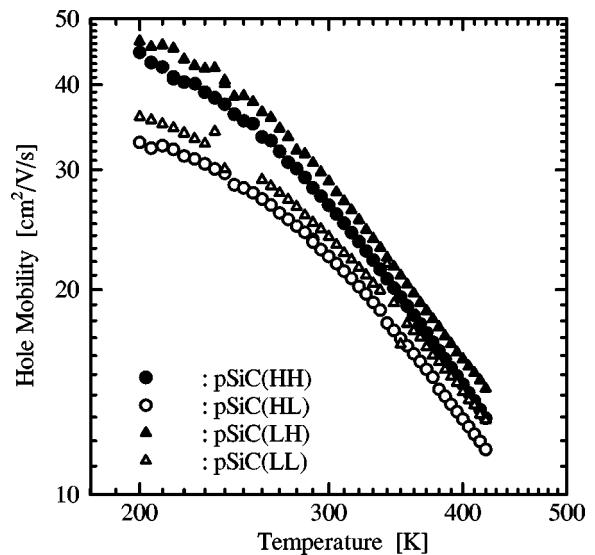


FIG. 3. Four temperature dependencies of hole mobility for sample preparation conditions with various implantation and annealing temperatures.

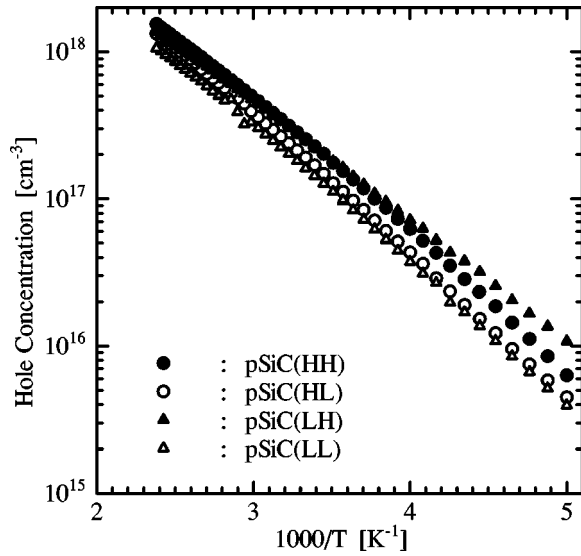


FIG. 4. Four temperature dependencies of hole concentration for sample preparation conditions with various implantation and annealing temperatures.

where  $m_h^*$ , which is required to calculate  $N_V(T)$  in Eq. (13), is assumed to be  $m_0$ .<sup>33</sup> The solid circles, open circles, solid triangles, and open triangles represent  $\Delta E_F(T)$  for  $p\text{SiC(HH)}$ ,  $p\text{SiC(HL)}$ ,  $p\text{SiC(LH)}$ , and  $p\text{SiC(LL)}$ , respectively. In the case of shallow dopants,  $\Delta E_F(T)$  increases monotonously with increasing  $T$ . In  $n$ -type SiC with  $N$  donors,  $\Delta E_F(T)$  increases monotonously with  $T$  in the temperature range of 80 and 420 K and  $\Delta E_F(T)$  is higher than the energy level of  $N$  donors.<sup>25,27</sup> In  $p$ -type SiC, however,  $\Delta E_F(T)$  decreases with increasing  $T$ , suggesting that the hole-occupation probability for the Al acceptor should be different from that for shallow dopants. Since  $\Delta E_F(T)$  is between 0.12 and 0.14 eV, moreover, the Fermi level is located be-

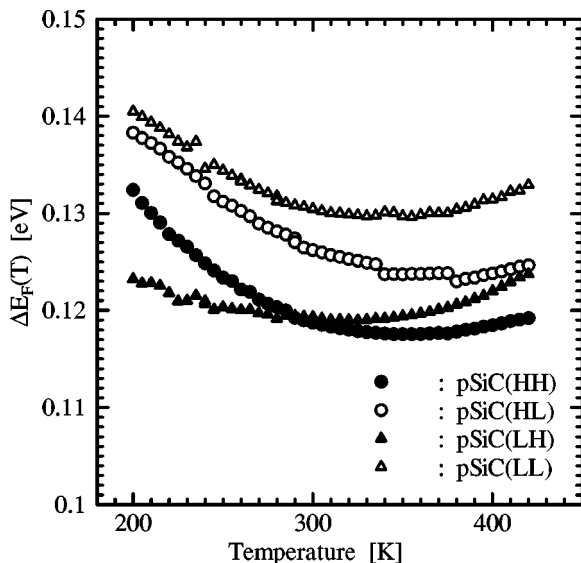


FIG. 5. Four temperature dependencies of Fermi level measured from  $E_V$  for sample preparation conditions with various implantation and annealing temperatures.

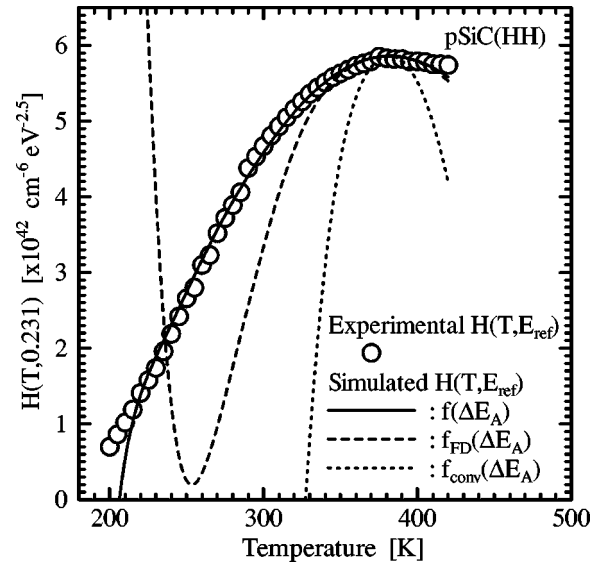


FIG. 6. Experimental  $H(T, E_{\text{ref}})$  (open circles) and three  $H(T, E_{\text{ref}})$  simulated with values determined by FCCS using  $f(\Delta E_A)$  (solid line),  $f_{\text{FD}}(\Delta E_A)$  (broken line), or  $f_{\text{conv}}(\Delta E_A)$  (dotted line).

tween  $E_V$  and  $\Delta E_A$  of  $\sim 0.18$  eV obtained from PL,<sup>9</sup> indicating that it should be impossible to ignore the influence of the excited states of the Al acceptor on  $p(T)$ .

## VI. DISCUSSIONS

### A. Distribution function suitable for Al in SiC

The open circles in Fig. 6 represent the experimental  $H(T, E_{\text{ref}})$  with  $E_{\text{ref}} = 0.231$  eV for  $p\text{SiC(HH)}$ . In the FCCS analyses,  $H(T, E_{\text{ref}})$  was calculated by interpolating  $p(T)$  with a cubic smoothing natural spline function at intervals of 0.1 K. The peak temperature and peak value of  $H(T, 0.231)$  are 381.8 K and  $5.86 \times 10^{42} \text{ cm}^{-6} \text{ eV}^{-2.5}$ , respectively. Since only one peak appears in the figure, it is considered that there is only one acceptor level in  $p\text{SiC(HH)}$ . Table II shows  $N_A$ ,  $\Delta E_A$  and  $N_{\text{comp}}$  determined by FCCS using  $f(\Delta E_A)$  or  $f_{\text{FD}}(\Delta E_A)$  or  $f_{\text{conv}}(\Delta E_A)$  from this peak.<sup>34</sup> In  $f(\Delta E_A)$  or  $f_{\text{conv}}(\Delta E_A)$ , the highest excited state considered in the FCCS analyses is the fourth excited state. Since  $\epsilon_s = 10$ , the excited state levels are estimated to be  $\Delta E_2 = 34.0$  meV,  $\Delta E_3 = 15.1$  meV,  $\Delta E_4 = 8.5$  meV, and  $\Delta E_5 = 5.4$  meV. All the  $\Delta E_A$  shown in Table II are close to  $\Delta E_A$  determined from PL. The value of  $N_A$  determined using  $f(\Delta E_A)$  is close to  $C_{\text{Al}}$ , while two  $N_A$  determined using  $f_{\text{FD}}(\Delta E_A)$  and  $f_{\text{conv}}(\Delta E_A)$  are much higher than  $C_{\text{Al}}$ ,<sup>35</sup> suggesting that  $f(\Delta E_A)$  is more appropriate for determining  $N_A$  from  $p(T)$  than the others.

TABLE II. Dependencies of results on distribution functions.

Distribution function	$N_A$ ( $\text{cm}^{-3}$ )	$\Delta E_A$ (meV)	$N_{\text{comp}}$ ( $\text{cm}^{-3}$ )
$f(\Delta E_A)$	$1.21 \times 10^{19}$	177	$2.29 \times 10^{17}$
$f_{\text{FD}}(\Delta E_A)$	$4.85 \times 10^{19}$	157	$2.45 \times 10^{18}$
$f_{\text{conv}}(\Delta E_A)$	$4.69 \times 10^{20}$	167	$1.62 \times 10^{19}$

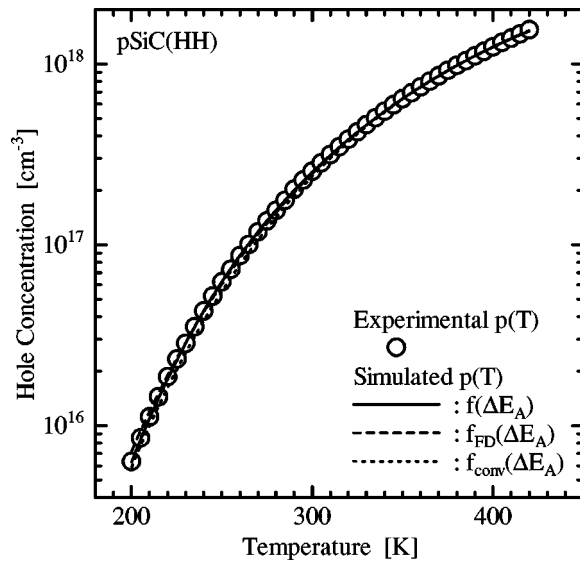


FIG. 7. Experimental  $p(T)$  (open circles) and three  $p(T)$  simulated with values determined by FCCS using  $f(\Delta E_A)$  (solid line),  $f_{FD}(\Delta E_A)$  (broken line), or  $f_{conv}(\Delta E_A)$  (dotted line).

Figure 6 also shows three  $H(T, E_{ref})$  simulated by Eq. (15) using  $N_A$ ,  $\Delta E_A$  and  $N_{comp}$  shown in Table II and  $\Delta E_F(T)$  obtained from Eq. (20) with the experimental  $p(T)$ . The solid, broken, and dotted lines represent the simulated  $H(T, E_{ref})$  for  $f(\Delta E_A)$ ,  $f_{FD}(\Delta E_A)$ , and  $f_{conv}(\Delta E_A)$ , respectively. Although all the peaks of the three simulated  $H(T, E_{ref})$  coincide with the peak of the experimental  $H(T, E_{ref})$ , the solid line is in agreement with the experimental  $H(T, E_{ref})$  better than the others. This indicates that  $N_A$ ,  $\Delta E_A$  and  $N_{comp}$  determined using  $f(\Delta E_A)$  are more reliable than the others.

Figure 7 shows the experimental  $p(T)$  (open circles) and three  $p(T)$  simulated by Eqs. (11) and (12) using  $N_A$ ,  $\Delta E_A$  and  $N_{comp}$  shown in Table II. The solid, broken, and dotted lines represent the simulated  $p(T)$  for  $f(\Delta E_A)$ ,  $f_{FD}(\Delta E_A)$ , and  $f_{conv}(\Delta E_A)$ , respectively. All the simulated  $p(T)$  are in good agreement with the experimental  $p(T)$ . This indicates that it is difficult to investigate the influence of the excited states of the acceptor on  $p(T)$  by the curve-fitting procedure of  $p(T)$ .

Figure 8 shows the experimental  $\Delta E_F(T)$  (open circles) and two simulated  $\Delta E_F(T)$ . Solid and broken lines in the figure correspond to  $f(\Delta E_A)$  and  $f_{FD}(\Delta E_A)$ , respectively. The solid line is in agreement with the experimental  $\Delta E_F(T)$  better than the broken line, which results in a coincidence of values between the experimental  $H(T, E_{ref})$  and the  $H(T, E_{ref})$  simulated using  $f(\Delta E_A)$ . Therefore, FCCS is considered to be an analysis method suitable for investigating the influence of the excited states of dopants more than the curve-fitting procedure of  $p(T)$ .

Figure 9 shows the influence of the excited states on  $p(T)$ . The open circles represent the experimental  $p(T)$ , and solid and broken lines represent  $p(T)$  simulated using  $f(\Delta E_A)$  and  $f_{FD}(\Delta E_A)$  with  $N_A = 1.21 \times 10^{19} \text{ cm}^{-3}$ ,  $\Delta E_A = 177 \text{ meV}$  and  $N_{comp} = 2.29 \times 10^{17} \text{ cm}^{-3}$ , respectively. From the figure, it is considered that the excited states of

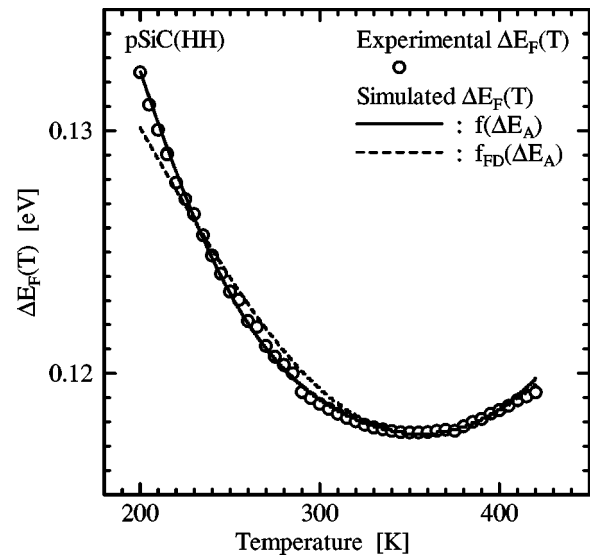


FIG. 8. Experimental  $\Delta E_F(T)$  (open circles) and two  $\Delta E_F(T)$  simulated with values determined by FCCS using  $f(\Delta E_A)$  (solid line) or  $f_{FD}(\Delta E_A)$  (broken line).

acceptors enhance the ionization efficiency of acceptors at high temperatures.

In Fig. 10, the solid, chain, and broken lines represent  $\Delta E_A(T)$ ,  $\Delta E_F(T)$ , and  $\exp(-E_{ex}(T)/kT)$ , respectively, which are simulated using  $N_A$ ,  $\Delta E_A$  and  $N_{comp}$  determined using  $f(\Delta E_A)$ .  $\Delta E_A(T)$  decreases with  $T$ , and then  $\Delta E_A(T)$  above 420 K becomes lower than  $\Delta E_F(T)$ , indicating that the ionization efficiency of the Al acceptors increases rapidly with  $T$ . In other words,  $\exp(-E_{ex}(T)/kT)$  decreases rapidly with  $T$ . In Eq. (2), the function

$$\sum_{r=2} g_r \exp\left(\frac{\Delta E_r - \Delta E_F(T)}{kT}\right) \quad (21)$$

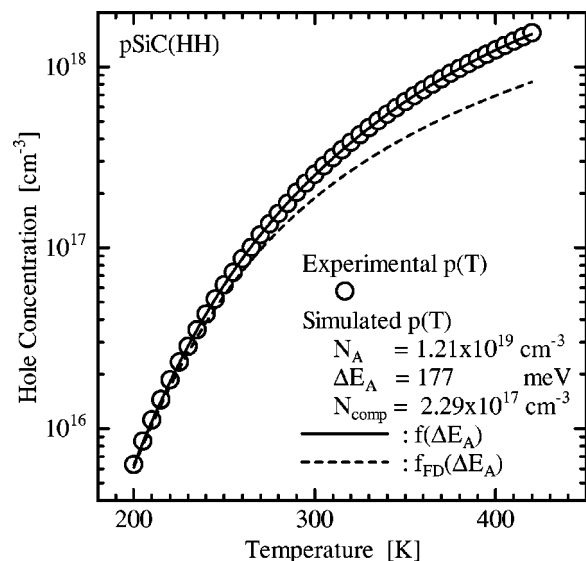


FIG. 9. Experimental  $p(T)$  (open circles) and two  $p(T)$  simulated using  $f(\Delta E_A)$  (solid line) or  $f_{FD}(\Delta E_A)$  (broken line). In the simulation, the values determined by FCCS using  $f(\Delta E_A)$  are used.

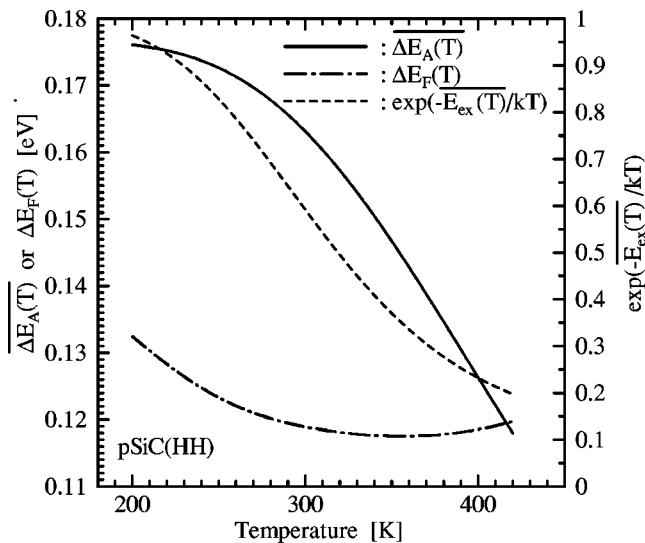


FIG. 10. Temperature dependencies of  $\overline{\Delta E_A(T)}$  (solid line),  $\Delta E_F(T)$  (chain line) and  $\exp(-E_{\text{ex}}(T)/kT)$ , which are simulated with  $N_A$ ,  $\Delta E_A$  and  $N_{\text{comp}}$  determined using  $f(\Delta E_A)$ .

signifies that the excited states behave just like a hole trap, while the function

$$\exp\left(-\frac{E_{\text{ex}}(T)}{kT}\right) \quad (22)$$

means that the holes bounded to the acceptors can easily be emitted to the valence band because the holes trapped at the excited states of acceptors can be thermally emitted more easily than those at the ground state. Therefore,  $N_A$  required to meet the experimental  $p(T)$  becomes the reasonable value in the case of  $f(\Delta E_A)$ .

When the simulated  $H(T, E_{\text{ref}})$  is similar to the experimental  $H(T, E_{\text{ref}})$ , the simulated  $p(T)$  is always fitted to the experimental  $p(T)$ . However, the opposite is not always true. This indicates that the curve-fitting procedure of  $p(T)$  is not suitable for investigating the influence of the excited states on the majority-carrier concentration. Moreover, it is found that not only the influence of the excited states but also  $E_{\text{ex}}(T)$  should be considered in the analysis of  $p(T)$  in a semiconductor including deep dopants.

## B. Effects of implantation temperature and annealing temperature

Table III shows  $N_A$ ,  $\Delta E_A$  and  $N_{\text{comp}}$  for  $p\text{SiC(HH)}$  or  $p\text{SiC(HL)}$  or  $p\text{SiC(LH)}$  or  $p\text{SiC(LL)}$ . All the obtained values are considered to be reliable, because all the  $N_A$  are less than or close to  $C_{\text{Al}}$  and because all the  $\Delta E_A$  are close to

TABLE III.  $N_A$ ,  $\Delta E_A$  and  $N_{\text{comp}}$  for samples with various  $T_{\text{implant}}$  and  $T_{\text{anneal}}$ .

Sample number	$N_A$ ( $\text{cm}^{-3}$ )	$\Delta E_A$ (meV)	$N_{\text{comp}}$ ( $\text{cm}^{-3}$ )
$p\text{SiC(HH)}$	$1.21 \times 10^{19}$	177	$2.29 \times 10^{17}$
$p\text{SiC(HL)}$	$9.49 \times 10^{18}$	187	$1.62 \times 10^{17}$
$p\text{SiC(LH)}$	$7.14 \times 10^{18}$	178	$6.64 \times 10^{16}$
$p\text{SiC(LL)}$	$5.44 \times 10^{18}$	183	$1.23 \times 10^{17}$

$\Delta E_A$  obtained from PL. Here, all the  $N_A$  determined using  $f_{\text{FD}}(\Delta E_A)$  and  $f_{\text{conv}}(\Delta E_A)$  are much higher than  $1 \times 10^{19} \text{ cm}^{-3}$ .

As is clear from Table III, almost all of implanted Al atoms are located at the substitutional sites in  $p\text{SiC(HH)}$ , while only an half of implanted Al atoms are at the substitutional sites in  $p\text{SiC(LL)}$ . By making a comparison between two  $N_A$  in  $p\text{SiC(HH)}$  and  $p\text{SiC(LH)}$ ,  $T_{\text{implant}}$  is effective in forming acceptors in SiC.

In Fig. 5, the shape of  $\Delta E_F(T)$  in  $p\text{SiC(HH)}$  resembles that in  $p\text{SiC(HL)}$ , while the shape in  $p\text{SiC(LH)}$  is like that in  $p\text{SiC(LL)}$ . Therefore, it is possible that  $T_{\text{implant}}$  affects the shape of  $\Delta E_F(T)$ . This may correlate with the dependence of  $\Delta E_A$  on  $T_{\text{implant}}$ , since  $\Delta E_A$  in the samples annealed at  $1575^\circ\text{C}$  are lower than  $\Delta E_A$  in the samples annealed at  $1443^\circ\text{C}$ .

## VII. CONCLUSION

Al-implanted  $p$ -type 4H-SiC layers with various  $T_{\text{implant}}$  and  $T_{\text{anneal}}$  were fabricated, and  $p(T)$  in those layers were obtained from Hall-effect measurements. Then,  $N_A$ ,  $\Delta E_A$  and  $N_{\text{comp}}$  were determined from  $p(T)$  using three kinds of distribution functions for acceptors. Since the Fermi level was located between the acceptor level and  $E_V$  in these samples, the proposed distribution function considering the influence of the excited states of dopants was found to be the most suitable for investigating the relationship between  $N_A$  and  $p(T)$  in Al-implanted  $p$ -type 4H-SiC. Moreover, it was demonstrated that the proposed FCCS could study this influence in detail, while the curve-fitting procedure of  $p(T)$  could not. When  $T_{\text{implant}} = 1000^\circ\text{C}$  and  $T_{\text{anneal}} = 1575^\circ\text{C}$ , almost all of implanted Al in 4H-SiC atoms was found to act as an acceptor.

## ACKNOWLEDGMENTS

The author would like to thank Dr. H. Sugimoto of the Mitsubishi Electric Corp. and Dr. K. Sekine of the Ion Engineering Research Institute Corp. for the sample preparation and RBS measurements. This work was partially supported by the Academic Frontier Promotion Projects of the Ministry of Education, Culture, Sports, Science and Technology, and it was also partially supported by the R&D Association of Future Electron Devices (FED) and the New Energy and Industrial Technology Development Organization (NEDO).

<sup>1</sup>P. Y. Yu and M. Cardona, *Fundamentals of Semiconductors: Physics and Materials Properties*, 2nd ed. (Springer, Berlin, 1999), p. 156.

<sup>2</sup>B. Sapoval and C. Hermann, *Physics of Semiconductors* (Springer, New York, 1993), p. 73.

<sup>3</sup>J. Singh, *Semiconductor Devices: An Introduction* (McGraw-Hill, New York, 1994), p. 110.

<sup>4</sup>E. Burstein, J. J. Oberly, J. W. Davisson, and B. W. Hennis, *Phys. Rev.* **82**, 764 (1951).

<sup>5</sup>E. Burstein, E. E. Bell, and J. W. Davisson, *J. Phys. Chem.* **57**, 849 (1953).

<sup>6</sup>A. Onton, P. Fisher, and A. K. Ramdas, *Phys. Rev.* **163**, 686 (1967).

<sup>7</sup>J. J. Rome, R. J. Spry, T. C. Chandler, G. J. Brown, B. C. Covington, and R. J. Harris, *Phys. Rev. B* **25**, 3615 (1982).

<sup>8</sup>D. W. Fischer and J. J. Rome, *Phys. Rev. B* **27**, 4826 (1983).

<sup>9</sup>M. Ikeda, H. Matsunami, and T. Tanaka, *Phys. Rev. B* **22**, 2842 (1980).

<sup>10</sup>P. Y. Yu and M. Cardona, in Ref. 1, p. 160.

<sup>11</sup>A. Schöner, N. Nordell, K. Rottner, R. Helbig, and G. Pensl, *Inst. Phys.*

- Conf. Ser.*, edited by S. Nakajima, H. Matsunami, S. Yoshida, and H. Harima (IoP Publishing, Bristol, 1996), Vol. 142, p. 493.
- <sup>12</sup>T. Troffer, M. Schadt, T. Frank, H. Itoh, G. Pensl, J. Heindl, H. P. Strunk, and M. Maier, *Phys. Status Solidi A* **162**, 277 (1997).
- <sup>13</sup>G. Pensl, European Conference on Silicon Carbide and Related Materials 2002, 1–5 September 2002 (to be published in Materials Science Forum); N. Schulze, J. Gajowski, K. Semmelroth, M. Laube, and G. Pensl, *Mater. Sci. Forum* **353–356**, 45 (2001).
- <sup>14</sup>H. Matsuura, *New J. Phys.* **4**, 12.1 (2002) [<http://www.njpp.org/>].
- <sup>15</sup>H. Matsuura, *Mater. Sci. Forum* **389–393**, 679 (2002).
- <sup>16</sup>D. J. Kim, D. Y. Ryu, N. A. Bojarczuk, J. Karasinski, S. Guha, S. H. Lee, and J. H. Lee, *J. Appl. Phys.* **88**, 2564 (2000).
- <sup>17</sup>B. Sapoval and C. Hermann, in Ref. 2, p. 112.
- <sup>18</sup>R. A. Smith, *Semiconductors*, 2nd ed. (Cambridge University Press, Cambridge, 1978), p. 92.
- <sup>19</sup>N. W. Ashcroft and N. D. Mermin, *Solid State Physics* (Harcourt, Philadelphia, 1976), p. 586.
- <sup>20</sup>S. M. Sze, *Physics of Semiconductor Devices*, 2nd ed. (Wiley, New York, 1981), p. 24.
- <sup>21</sup>K. F. Brennan, *The Physics of Semiconductors with Applications to Optoelectronic Devices* (Cambridge University Press, Cambridge, 1999), p. 277.
- <sup>22</sup>P. Y. Yu and M. Cardona, in Ref. 1, p. 162.
- <sup>23</sup>H. Matsuura and K. Sonoi, *Jpn. J. Appl. Phys., Part 2* **35**, L555 (1996).
- <sup>24</sup>H. Matsuura, Y. Uchida, T. Hisamatsu, and S. Matsuda, *Jpn. J. Appl. Phys., Part 1* **37**, 6034 (1998).
- <sup>25</sup>H. Matsuura, T. Kimoto, and H. Matsunami, *Jpn. J. Appl. Phys., Part 1* **38**, 4013 (1999).
- <sup>26</sup>H. Matsuura, Y. Uchida, N. Nagai, T. Hisamatsu, T. Aburaya, and S. Matsuda, *Appl. Phys. Lett.* **76**, 2092 (2000).
- <sup>27</sup>H. Matsuura, Y. Masuda, Y. Chen, and S. Nishino, *Jpn. J. Appl. Phys., Part 1* **39**, 5069 (2000).
- <sup>28</sup>S. M. Sze, in Ref. 20, p. 18.
- <sup>29</sup>J. P. Biersack and L. Haggmark, *Nucl. Instrum. Methods* **174**, 257 (1980). The SRIM software for Windows OS can be downloaded at the website (<http://www.srim.org/>).
- <sup>30</sup>G. L. Harris, *Properties of Silicon Carbide*, edited by G. L. Harris (INSPEC, London, 1995), p. 3.
- <sup>31</sup>S. M. Sze, in Ref. 20, p. 34.
- <sup>32</sup>F. Szmulowicz, *Phys. Rev. B* **28**, 5943 (1983).
- <sup>33</sup>S. Yoshida, in Ref. 30, p. 69.
- <sup>34</sup>In the case of  $\gamma_H = 1.18$  the values of  $N_A$  for  $f(\Delta E_A)$  and  $f_{FD}(\Delta E_A)$  are  $1.62 \times 10^{19}$  and  $6.64 \times 10^{19} \text{ cm}^{-3}$ , respectively, while in the case of  $\gamma_H = 0.7$  the values of  $N_A$  for  $f(\Delta E_A)$  and  $f_{FD}(\Delta E_A)$  are  $6.79 \times 10^{18}$  and  $2.54 \times 10^{19} \text{ cm}^{-3}$ , respectively. The values of  $\Delta E_A$  are the same as those in Table II.
- <sup>35</sup>In order to obtain  $N_A$  close to  $C_{Al}$  using  $f_{FD}(\Delta E_A)$ ,  $\gamma_H$  should be decreased from 0.97 at 200 K to 0.54 at 420 K. The values of  $\gamma_H$  at high temperatures seem too small.